ENHANCED ADSORPTION OF CATIONIC AND ANIONIC DYES VIA LIGAND-INDUCED DEFECTS IN HKUST-1 ANALOGUES

Andrea R. Kelley†, J. Warmbrod*, J. Short*, M. Canine*, J. Cianfaglione*, J. Delp*, C. Ferguson*, J. Good*, J. Hernandez*, K. Hong*, A. Lambert-Conohan*, M. Steel*, B. Stephens*, D. Tran*, E. Trost-Rekich*, T. Wimsett*, S. Akinrelere*, P. Benfield*, J. Blevins*, S. Fernando*, W. Grimes*, H. Johnston*, E. Kim*, S. McCormick, S.*, P. Ramirez, P.*, S. Ronnie, S.*, Schneider, D.*, Shelton, H.*, Ulery, M.*, Young, K.*, Barba, B.*, C. Bray*, C. Cannedy*, S. Cody*, D. Cox*, Z. Garcia*, J. Guerrero*, J. Haymond*, M. Hayslett*, C. Jett*, J. Ko*, R. Luinstra*, D. Ritter*, A. San Agustin*, T. Tuffile*, T. Williams-Mitchel*, Brown*, T. Crow*, M. Farkas*, K. Freeman*, H. Hartz*, O. Honaker*, A. Jabour*, C. Johnson*, A. Kosinski*, S. Loos*, J. Lupian*, V. Peck*, E. Ramos*, O. Rubio*, B. Salinas* and Barry W. Hicks

Department of Chemistry, United States Air Force Academy, Colorado Springs, CO 80840

Abstract

Metal-organic frameworks (MOFs) are porous crystalline materials with exceptionally high surface areas, recognized by the 2025 Nobel Prize in Chemistry. A common MOF, HKUST-1, made from copper(II) cations and benzene-1,3,5-tricarboxylic acid (BTC) ($Cu_3(BTC)_2$) remains a benchmark for adsorption research, but its performance is limited by its pore geometry. In this study, three mixed-ligand MOFs (ML-MOFs) were synthesized by substituting 0.25 mole fraction of three alternative carboxylic acids: cyclohexane-1,3,5-tricarboxylic acid (CTC), benzene-1,2,4-tricarboxylic acid isomer (iBTC), or 1,4-benzenedicarboxylic acid (BDC). The adsorption capacities (q_c) of these ML-MOFs were evaluated using cationic methylene blue (MB) and various anionic diazo dyes. All ML-MOFs outperformed the HKUST-1 control in pollutant removal. Specifically, the BDC-modified ML-MOF exhibited the highest capacity for MB, while the iBTC-modified framework showed superior performance for anionic dyes. Although all frameworks showed a preference for cationic species, the enhanced performance of ML-MOFs suggests that ligand-induced structural defects (which may potentially alter pore geometries) may significantly improve adsorption efficiency.

†Corresponding author: Andrea.Kelley@afacademy.af.edu *Undergraduate researchers and co-authors

Keywords: metal-organic frameworks, dye adsorption
Received: May 9, 2026 Accepted: May 11, 2026 Revision received: May 22, 2026 Published: May 29, 2026

Introduction

Metal-organic frameworks (MOFs) are porous crystalline materials formed by connecting metal-containing nodes with organic linkers, creating open lattice-like structures with high surface area, tunable pore sizes, and large pore volumes[1,2]. Because of these structural features, MOFs have become important multifunctional materials in chemistry, with applications in gas storage, molecular separation, catalysis, sensing, drug delivery, and pollutant removal[3-8]. Their significance was further recognized when Susumu Kitagawa, Richard Robson, and Omar M. Yaghi received the 2025 Nobel Prize in Chemistry "for the development of MOFs," highlighting the major impact MOFs have had on modern materials chemistry and sustainability research[9]. One reason MOFs are so valuable is that their specificity can be adjusted through ligand design, mixed-ligand MOFs (ML-MOFs), post-synthetic modification, and MOF-on-MOF hybrid structures, allowing researchers to tailor them for specific chemical functions[10-12]. This flexibility is especially useful in environmental applications, where MOFs have been studied for removing dyes and other pollutants from aquatic environments[13]. One of the most well-studied MOFs, with scores of papers describing dozens of successful synthetic strategies, including some approachable by first year undergraduates or even high school students, is HKUST-1[14-17]. It is made from copper(II) cations and benzene-1,3,5-tricarboxylic acid (BTC) linkers with a stoichiometry of ($Cu_3(BTC)_2$). Moreover, hybrid magnetic HKUST-1 MOFs have shown strong adsorption performance for Congo red dye, while newer work has explored mixed-ligand MOFs for targeting and degrading organic dyes in aqueous media[18,19], indicating that there are a lot of areas for ML-MOF research open to pursuit with HKUST-1 analogs. Current MOF research continues to expand through advanced structures such as MOF-on-MOF core-shell heterostructures for propane/propylene separation and machine-learning-guided optimization for carbon capture and photocatalytic conversion[20, 21]. Therefore, synthesizing and testing mixed-ligand MOFs against multiple dyes is important because it allows researchers to evaluate how structural design influences adsorption, selectivity, and pollutant-removal efficiency for potential future applications. In this work, three ML-MOFs were compared to the control HKUST-1 for their adsorption of both cationic and anionic dyes (Scheme 1).

Materials & Methods

Materials used and sources

The BTC, copper(II) acetate monohydrate, 2-naphthol,

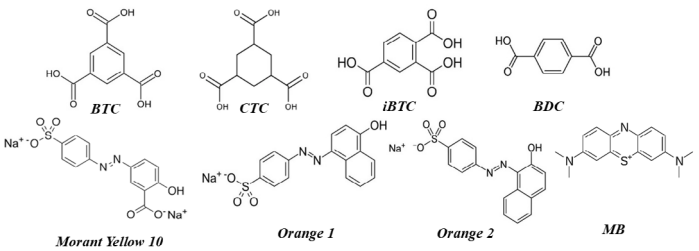

Scheme 1. Structures of ligands used to make ML-MOFs (top row) and dyes used to test them (bottom row). Top row (left to right): Trimesic Acid (BTC), Cyclohexane-1,3,5-tricarboxylic Acid (CTC), Benzene-1,2,4-tricarboxylic Acid (iBTC), Terephthalic Acid (BDC). Bottom row (left to right) Mordant Yellow 10, Orange 1, Orange 2, and MB.

1,4-benzenedicarboylic acid (BDC) and sulfamic acid were purchased from Aldrich. The 1-naphthol, dimethylformamide (DMF), ethanol, and sodium salt of 4-(2-hydroxyethyl)-1-piperazineethanesulfanic acid (HEPES) sodium salt were purchased from Sigma-Aldrich. The salicylic acid was purchased from Alfa Aesar. The methylene blue (MB) was purchased from Baker. The hydrochloric acid (HCl) was purchased from Fisher. The benzene-1,2-4-tricarboxylic acid isomer (iBTC) was purchased from Oakwood Chemical. The cyclohexane-1,3,5-tricarboxylic acid (CTC) was purchased from Ambeed. Equipment used included a Sorvall Lynx 6000 centrifuge with a swinging bucket rotor, a Varian Bio50 spectrometer, and a Binder Drying oven.

Diazo Dye Synthesis

Aminobenzenesulfonic acid (0.0025 mol) was combined with 2.0 mL of 2.75 M Na_2CO_3 in a 50-mL plastic tube and stirred until fully dissolved. A solution of sodium nitrite (0.00275 mol) in 4.0 mL of deionized water was added dropwise with continuous stirring to afford a homogeneous mixture. The reaction mixture and a separate solution of 3.0 M HCl (7.0 mL, 0.021 mol) were cooled in an ice bath to below 5 °C, as monitored by thermometer. The cold HCl solution was then added dropwise to the reaction mixture over approximately 2 min while maintaining the temperature below 5 °C. After complete addition, the reaction mixture was stirred for an additional 5 min under the same temperature conditions. For the diazonium coupling reactions, the phenolic coupling reagent (0.00255 mol) was dissolved in 6 mL of 1 M sodium hydroxide in a 50-mL Erlenmeyer flask, with mild heating applied if necessary to aid dissolution. The solution was subsequently cooled in an ice bath and stirred continuously while the freshly prepared diazonium salt solution was added dropwise over 2–3 min. Upon completion of the addition, 3 M HCl was added dropwise until the pH reached approximately 3, as indicated by the formation of a precipitate. The resulting sodium salt of the anionic diazo dyes were collected by vacuum filtration, washed with 10 mL of deionized water, and allowed to dry until the following laboratory period. The mass of the dried product was then measured to determine the percent yield, which ranged from about 20-80%.

Diazo Dye Characterization

The diazo dyes were characterized by thin-layer chromatography (TLC), UV–visible spectroscopy, and qualitative textile dyeing studies to evaluate their purity, optical behavior, and substrate affinities. TLC was used as an initial assessment of product homogeneity, since a single well-defined spot would be expected for a pure component, whereas multiple spots or streaking would indicate the presence of impurities, side products, or multiple dye-related species. A methanolic solution of the dye was spotted alongside precursor standards, developed in a butanol, acetic acid, and methanol (6:1:1) mobile phase, and visualized under ultraviolet illumination after a 20-min solvent evaporation period. Figure 1 shows representative TLC plates for the three dyes. UV–visible spectroscopy was employed to determine the adsorption profile of the dye under different solution conditions and to identify the wavelength of maximum absorbance, providing information about the extent of conjugation and the effect of protonation state on the electronic structure of the chromophore. The halochromic properties of the dye were analyzed by collecting ultraviolet-visible (UV-Vis) absorbance spectra (400–700 nm) of samples dissolved in highly acidic (HCl), highly basic (NaOH), and pH-controlled (phosphate buffer pH 7) environments. In addition, a fabric strip containing 13 different fabric types was exposed to the dye solution as a qualitative test of dye uptake, allowing comparison of relative dye–fiber interactions across a range of textile substrates. Figure 2 shows representative dyed fabric strips. Collectively, these characterization methods confirmed formation of a strongly absorbing colored product and provided evidence regarding their purity, solution-phase optical properties, and affinities for polymeric matrices with different charges. Finally, to quantify the

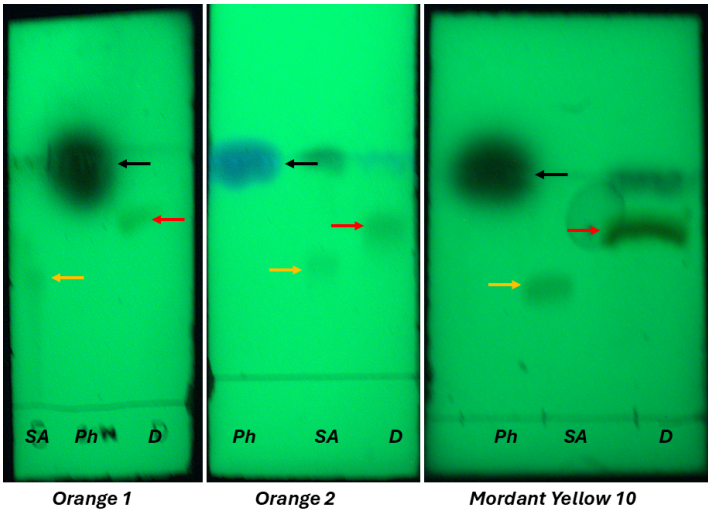

Figure 1. Thin-Layer Chromatography Analysis of Synthetic Dye Products. Standardized silica TLC plates showing the diazo dye products. Spotted samples include starting reagents sulfanilic acid (SA, yellow arrows) and phenols (Ph, black arrows), alongside the purified dye products (D, red arrows). Consistent with the excess phenol stoichiometry used in the coupling reaction, residual phenol is visible in the Orange 2 and Mordant Yellow 10 lanes, while sulfanilic acid is fully consumed across all samples. In this representative Orange 1 sample, nearly complete removal of the 1-naphthol was observed.

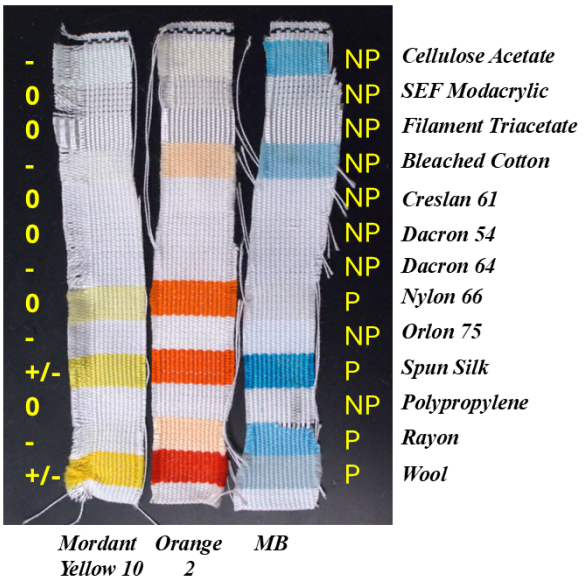

Figure 2. Multi-fabric test strips stained with three of the dyes used in this work (strips stained with orange 1 were very similar to those stained with orange 2).The charge on the fabric polymer, positive (+), negative (-), neutral (0), or zwitterionic (+/-) is indicated on the left in yellow, while the polarity is indicated on the right in yellow. The protein fabrics (silk and wool) bound all types of dye well. The polymers that stained best with anionic diazo dyes were nylon 6,6 and to a lesser extent, cotton and rayon. The polymers that bound MB selectively were negatively charged including cellulose acetate and rayon.

dye's concentration-dependent optical behavior, a concentrated stock solution prepared in a HEPES buffer was subjected to sequential volumetric dilutions to generate a standardized working solution. Six subsequent serial dilutions were prepared (0, 2, 4, 6, 8, 10 μM) and their corresponding absorbance spectra were measured to construct a Beer's Law standard calibration curve. This last analysis was repeated using a stock solution of MB and equivalent dilutions.

MOF Synthesis

MOF synthesis and testing were modified from Wang and Liu (16). A copper(II) acetate solution was prepared by dissolving 0.000456 mol copper(II) acetate monohydrate in 10 mL of 10% DMF in water, stirred at 50 °C. Separately, a linker solution was prepared by dissolving 0.000676 mol trimesic acid (BTC) and a 0.25 mol fraction of the various ML-MOF ligands (CTC, iBTC, or BDC) in 20 mL EtOH containing 10% DMF. Although BTC, CTC and iBDC are sufficiently soluble in EtOH, the BDC is notoriously insoluble, requiring DMF; for consistency DMF was added to the other ML-MOFs as well. The linker solution was added dropwise to the copper(II) solution over 10 min at 50 °C to ensure all ML carboxylic acids remained soluble. The mixtures were then covered and stirred at 60 °C for 50 min. The mixtures containing the products were divided into two 15-mL centrifuge tubes and spun in the centrifuge in a swinging bucket rotor at 5000 rpm for 5 min. After decanting, each pellet was resuspended in 5 mL ethanol (EtOH), combined into a single tube, and washed twice with 100% EtOH. The final pellet was resuspended in 1-2 mL of 100% EtOH and transferred to a pre-weighed glass vial. The products were dried 12 h at 100 °C, then 24 h at 135 °C to remove all solvents. Yields ranged considerably (0-80%), but overall average yields were about 40-60%.

MOF Testing

A 10 μM MB solution was prepared by transferring 10.5 mL of a 20 μM stock solution (in 250 μM HEPES buffer, pH 7.0) into a 50-mL conical tube and adding 10.5 mL of 250 μM HEPES buffer for a total volume of 21.0 mL. The solution was mixed well, and a 1.0 mL portion was placed into a 1 cm cuvette to be used as the untreated control sample. The same procedure was repeated to prepare the diazo dye control sample. For the adsorption experiments, about 10 mg of MOF was weighed into each of two 50-mL centrifuge tubes using an analytical balance and exact masses recorded. One tube was filled with the MB solution, and the other was filled with the various diazo dyes. Both tubes were capped and sonicated for 5–10 s to disperse the MOF particles. The mixtures were then placed on a rocker and allowed to equilibrate for 60 min. After equilibration, the tubes were centrifuged for 5 min to separate the MOF solids from the solution. A few mL of the solutions from each tube were carefully transferred into clean 15 mL tubes, making sure no solid particles were carried over. Visible absorbance spectra were then collected from 400 to 700 nm for each sample. Using the initial solution volume (20.0 mL), the molecular weight of the dye, and the measured MOF mass, the adsorption capacity (q_e) of the MOF was determined.

Results

Figure 3 shows a digital image taken during the experiment showing how the MOF colors change. The powder blue mixture in the 50-mL tube is the MOF post synthesis, the middle vial shows the MOF after being heated at 100 °C for 12 h, and the right vial is the MOF after being heated at 135 °C for 24 h. Post synthesis, the color of blue varies from a teal shade to a dark navy or purple which is a well-documented change in HKUST-1 in response to loss of various solvents (EtOH, water, and DMF) as the temperature is increased. Interestingly, the ML-MOF made from the BDC was more of a navy color compared to the more purple color of the other ML-MOFs. Consistent with formation of MOFs, at least under the light microscope, the dried solids appeared to be crystalline rather than amorphous powders, and they were found to absorb water in a humid environment at levels comparable to those previously published[22] (data not shown).

Figure 4 demonstrates the visible absorbance spectra of the four dyes tested using MOFs: MB, mordant yellow 10, orange 1, and orange 2. Mordant yellow 10 does not show a clear maxi-

Figure 3. A digital image showing the various stages of the MOF preparation. After the 60 min incubation during the synthesis of carboxylate ligands with copper(II) ions a powder blue mixture was obtained. The partially dried MOFs retained a similar color after incubation at 100 °C (middle vial) which removed ethanol and some of the water. After incubation at 135 °C for 24 h, all water and DMF were removed resulting in dark navy blue-purple solid (right vial).

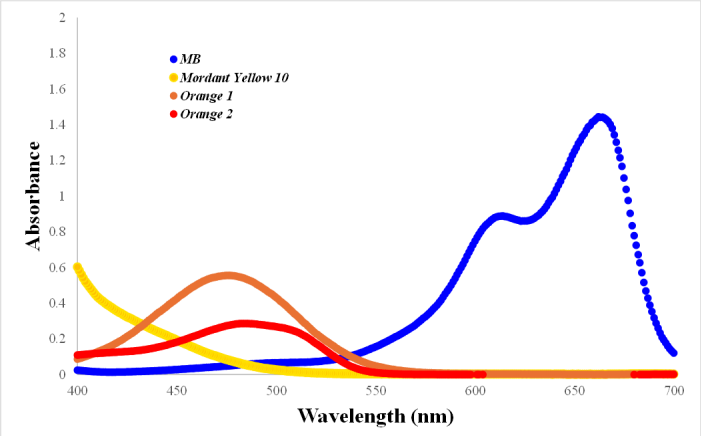

Figure 4. Visible absorbance spectra of all four dyes used in this work at 20 mM. MB has the most red-shifted spectrum and the highest absorbance, while yellow mordant 10 does not show an absorbance maximum in the visible range. For that reason, 400 nm was used for all quantitation of yellow mordant 10.

mum in the visible range, appearing to peak in the UV. Orange 1 and 2 have similar λ_{max} values, and both have considerably lower absorbance values than MB. Full spectra were collect to construct standard curves at the λ_{max} in the visible range (400-700 nm).

Standard Beer's Law curves from representative student data for each of the four dyes are shown in Figure 5. All data were well fit by straight lines with high correlation coefficients. The wavelengths of maximum adsorbance and the molar extinction coefficient values for each of the dyes with absorption max in the visible are close to other published values[23-25]. For mordant yellow 10, since quartz cuvettes were not available, 400 nm, the highest absorbance in the visible was used, and at that wavelength the molar extinction coefficient was similar to that of orange I (see Fig. 4).

Figure 6 shows a representative data set from one student group for the MOF adsorption experiments. The absorbance spectrum for 20 μM MB untreated control shows a maximum absorbance of about 0.9, and a much smaller value in the treated sample, which also shows a slight shift λ_{max}. The MOF-treated sample has a significantly smaller absorbance; the relative concentrations were determined using the standard curves (Fig. 5). The same observations were seen using the diazo dye (orange 2 in this sample), but the percent of dye absorbed were much smaller relative to the untreated controls. The dye concentrations in both samples were quantified using the standard curves similar or identical to those in Fig. 5.

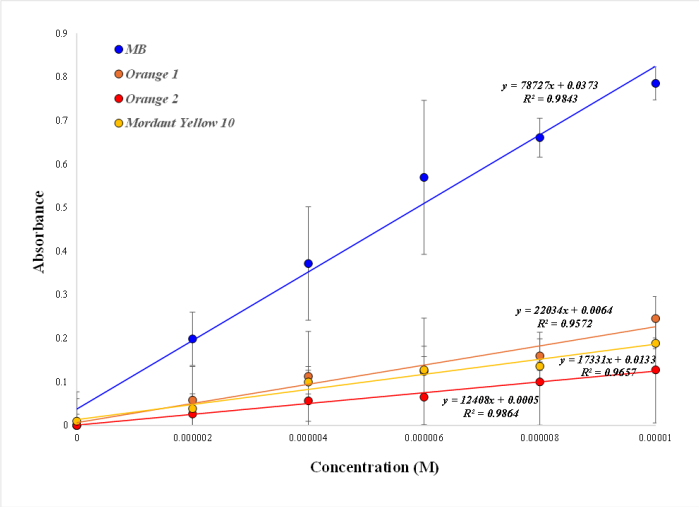

Figure 5. Representative Beer's Law standard curves of absorbance versus wavelength for all four dyes. MB had a significantly larger slope due to its higher molar extinction coefficient. Plotted values represent the mean absorbance from three student groups with error bars plotted as standard deviations.

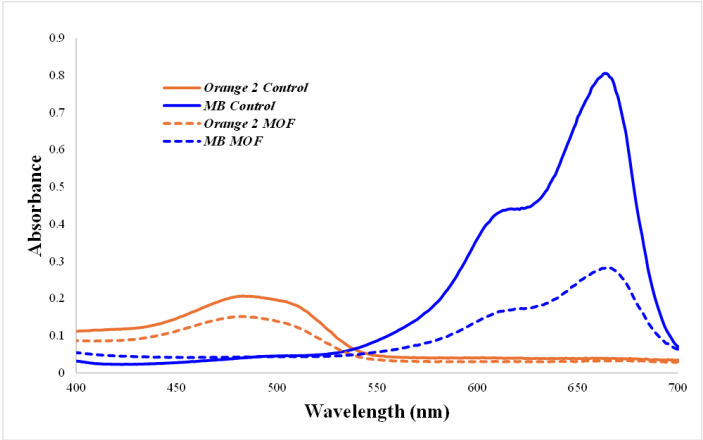

Figure 6. Representative student data for the MOF adsorption experiments. These absorbance spectra are for MB and orange 1 incubated with and without the CTC ML-MOF. For both the MB and the diazo dyes, the MOF treated samples had lower absorbance values than the untreated controls, although the percent difference was much greater for MB than for the diazo dyes.

Figure 7 displays the adsorption capacity (q_c) in mg dye/g MOF for each of the tested ML-MOFs using each of the four dyes. It was already confirmed by dying the fabric strip with all four dyes, that cationic dyes interacted better with anionic polymers and vice versa (data not shown). These results indicate that while all the ML-MOFs had a greater adsorption capacity for MB, only the ML-MOF made from BDC was statistically significantly different than the HKUST-1 control. Among the ML-MOFs, BDC had the highest adsorption for MB, and iBTC demonstrated the highest overall capacity for the diazo dyes. Regardless of the MOF used, MB consistently showed stronger adsorption than the diazo dyes.

Discussion

Dye and ML-MOF synthesis were effectively accomplished, albeit with yields lower than comparable published values. Across all tested materials, the ML-MOFs exhibited a significantly higher adsorption capacity (q_c) than the control, with the iBTC ML-MOF demonstrating the highest overall performance. The values are less than true maximal loading values at equilibrium, (Q_c) values because we worked at lower dye concentrations and used shorter incubation periods that may not have allowed full equilibrium to have been reached. Nevertheless, our q_c values are very comparable or superior to those in previously published work[16,26]. In addition, since our diazo dyes were synthesized in highly acidic solutions, to ensure they were anionic rather than neutral, we did the adsorption experiments in 250 mM HEPES buffer, and although it is a zwitterionic buffer it likely competed with the dyes for adorption. Regardless of the specific MOF utilized, MB was

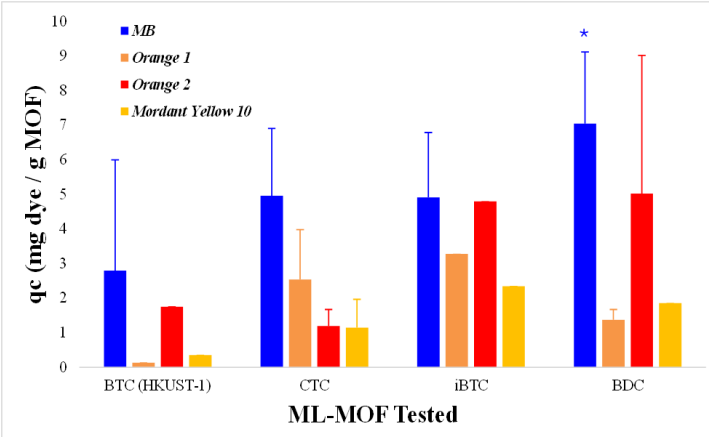

Figure 7. A graph of adsorption capacity versus ML-MOF type for each of the four dyes. The mixed ligand MOFs have a greater adsorption capacity than the adsorption capacity for the control MB dye. All four MOFs (BTC, CTC, iBTC, BDC) appear to have greater adsorption capacity for the cationic MB than for the anionic diazo dyes. Error bars represent the standard deviation from triplicate data points, and bars with no errors are the average of duplicate determinations. The asterisk indicates that the BDC ML-MOF adsorption of MB is significantly different (determined by an unpaired student T-test) than the control HKUST-1 MOF ($P < 0.05$).

consistently identified as the most effectively adsorbed dye. Ultimately, every ML-MOF outperformed the control (except in the case of CTC average adsorption capacity for Orange 2 compared to BTC; statistical analysis makes it difficult to make the claim for the specific makeup), indicating that ML-MOFs should be considered for any application where MOFs might be applied.

That mixed-ligand MOFs demonstrated enhanced dye adsorption compared to standard HKUST-1 is possibly due to the defect-induced active sites caused by the incorporation of the alternative carboxylates that may have altered both pore windows and pore sizes in the MOF networks. It is likely that standard HKUST-1 is limited by comparatively smaller pore windows that hinder diffusion of the dyes. This conclusion is supported by the increase not only in cationic MB adsorption, but also in anionic dye adsorption by the ML-MOFs, which might minimize electrostatic repulsion. Also, the yellow mordant 10 dye, which is a dianion, would be expected, as seen, to have the lowest adsorption. Our results also suggest that the cyclohexane-based MOF (CTC) had the smallest benefit, likely because its non-planar, flexible backbone is less effective at increasing pore size. Also, BDC, which probably caused the most significant alteration of the base HKUST-1 structure was the most effective ML-MOF we produced. Taken together, our results suggest that virtually any application of MOFs might be improved by finding the correct ML-MOF to substitute in its place.

Structurally, the ML-MOFs did not absorb the anionic dyes as well as the cationic MB. This is likely because the ML-MOFs have a naturally negative surface charge, which causes electrostatic repulsion with the negatively charged anionic dyes. Additionally, to improve the adsorption of anionic dyes, we could modify the ML-MOF by adding positively charged functional groups to the carboxylate linkers. Likely candidates include protonated amines, pyridinium groups, imidazolium groups, and especially quaternary ammonium groups, which retain a permanent positive charge in aqueous solution. Adding cationic functional groups such as these would give the MOF localized positive charges, creating an electrostatic attraction for anionic dyes[27]. Furthermore, the more electropositive ML-MOFs could be highly effective not just for removing anionic dyes, but also for cleaning up other negatively charged environmental pollutants, such as pesticides, herbicides, and "forever chemicals" like PFAS and PFOAs.

Acknowledgements

We would like to thank the USAFA Department of Chemistry and the Research Center for funding of this work. We also wish to thank Abby Jennings for reviewing the manuscript and providing suggestions for improvement. All undergraduate authors contributed equally to data collection and manuscript preparation. Draft writing was done without the aid of AI, but Google Gemini was used to make initial edits; the final draft was written without AI and reviewed by all authors. The views expressed in this article are those of the authors and do not necesssarily reflect the official policy or position of the United States Air Force Academy, the Air Force, the Department of Defense, or the U.S. Government.

References

1. Zafar, F. and Sharmin, E., editors. *Metal-Organic Frameworks*. *IntechOpen*, 2016.
2. Zhou, H.-C.J. and Kitagawa, S. *Chemical Society Reviews*, 2014, *43 n16*, 5415–5418.
3. Jiao, L.; et al. *Chem. Soc. Rev.*, 2019, *48 n.7*, 1925–1978.
4. Li, B.; Wen, H.-M.; Zhou,W; Chen, B.. "*J. Phys. Chem. Let.*, 2014, *5 n20*, 3468–3479.
5. Pettinari, C.; et al. *Polymer International*, 2017, *66 n6*, 731–744.
6. Kuppler, R.J.; et al. *Coord. Chem. Rev.*, 2009, *253 n23*, 3042–3066.
7. Horcajada, P.;, et al. *Chem. Rev.*, 2011, *112 n2*, 1232–1268.
8. Ma, S. and Zhou, H.-C. *Chem. Comm.*, 2010, *44*, 44–53.
9. Nobel Prize Outreach. "The Nobel Prize in Chemistry 2025." *NobelPrize.org*, 2025. URL: https://www.nobelprize.org/prizes/chemistry/2025/summary/?utm_source=chatgpt.com accessed May 2026.
10. Kitagawa, S.: Kitaura, R.; Noro, S. *Angewandte Chem. Intern. Ed.*, 2004, *43 n18*, 2334–2375.
11. Yaghi, O. M.; et al. *Nature*, 1999, *402 n6759*, 276–279.
12. Liu, C.; et al. *Coord. Chem. Rev.*, 2021, *432*, 213743.
13. Beydaghdari, M.; et al. *Energies*, 2022, 15, 2023.
14. Yang, L.; et al. *J. Mat. Chem. B,* 2024*, 12.11*, 2670-2690.
15. Omertassov, D.D.; et al. *ACS Omega,* 2025 10.28, 30259-30271.
16. Wang, X. and Liu, Y. *J. Chem. Ed.,* 2025*, 102.11*, 4840-4846.
17. Lee, K. and Lee, S. *Inter. J. of High School Res., 2024,* 6.1.
18. Xu, Y.; et al. *RSC Adv.,* 2015*, 5 n25*, 19199–19202.
19. Talha, K.; et al. *RSC Adv*, 2021, 11 n38, 23838-23845.
20. Peng, J.; Wang, Z.; Geng, N.; et al. *Small,* 2026, e73200.
21. Sundararaman, S.; et al. *Results Eng.* 2026, 110704.
22. Schoenecker, P. M.; et al. *Ind. Eng. Chem. Res.* 2012, *51*, 6513–6519.
23. Bergmann, K.; O'Konski, C. T. *J. Phys. Chem.* 1963, *67*, 2169–2177.
24. Oakes, J.; Gratton, P. *J. Chem. Soc., Perkin Trans. 2,* 1998, *12*, 2563–2568.
25. Taniguchi, M.; Lindsey, J. S. *Photochem. Photobiol.* 2018, *94*, 290–327.
26. Cheng, Y.; Shi, D.; Yuan, Y. D.; Zhao, D. *J. Chem. Educ.* 2020, *97*, 4145–4151.
27. Xie, X.; et al. *ACS Omega,* 2020, *5*, 13595–13600.